Contrib Mineral Petrol (1995) 122:322–335

E. Hegner · H.J. Walter · M. Satir

Pb-Sr-Nd isotopic compositions and trace element geochemistry of megacrysts and melilitites from the Tertiary Urach volcanic field: source composition of small volume melts under SW Germany

Received: 9 March 1995 / Accepted: 24 July 1995

Abstract The Urach volcanic field is unique within the Tertiary–Quaternary European volcanic province (EVP) due to more than 350 tuffaceous diatremes and only sixteen localities with extremely undersaturated olivine melilitite. We report representative Pb-Sr-Nd isotopic compositions and incompatible trace element data for twenty-two pristine augite, Cr-diopside, hornblende, and phlogopite megacryst samples from the diatremes, and seven melilitite whole rocks. The Pb isotopic compositions for melilitites and comagmatic megacrysts have very radiogenic $^{206}Pb/^{204}Pb$ ratios of 19.4 to 19.9 and plot on the northern hemisphere mantle reference line (NHRL). The data indicate absence of an old crustal component as reflected in the high $^{207}Pb/^{204}Pb$ ratios of many basalts from the EVP. This inference is supported by $^{206}Pb/^{204}Pb$ ratios of $\sim$17.6 to 18.3 and ε_{Nd} of ~ -7.8 to $+1.6$ for five phlogopite xenocryst samples reflecting a distinct and variably rejuvenated lower Hercynian basement. The $^{87}Sr/^{86}Sr$ ratios of 0.7033 to 0.7035 in the comagmatic megacrysts are low relative to their moderately radiogenic Nd isotopic compositions (ε_{Nd} $+2.2$ to $+5.1$) and consistent with a long-term source evolution with a low Rb/Sr ratio and depletion in light rare-earth elements (LREE). The melilitite whole-rock data show a similar range in Nd isotopic ratios as determined for the megacrysts but their Sr isotopic compositions are often much more radiogenic due to surface alteration. The REE patterns and incompatible trace element ratios of the melilitites (e.g. Nb/Th, Nb/U, Sr/Nd, P/Nd, Ba/Th, Zr/Hf) are similar to those in ocean island basalts (OIB); negative anomalies for normalized K and Rb concentrations support a concept of melt evolution in the lithospheric mantle. Highly variable Ce/Pb ratios of 29 to 66 are positively correlated with La/Lu, La/K_2O, and Ba/Nd and interpreted to reflect melting in the presence of residual amphibole and phlogopite. The data suggest an origin of the melilitites from a chemical boundary layer very recently enriched by melts from old OIB sources. We suggest that the OIB-like mantle domains represent low-temperature melting heterogeneities in an upwelling asthenosphere under western Europe.

E. Hegner (✉) · H.J. Walter[1] · M. Satir
Institut für Mineralogie, Petrologie und Geochemie, Universität Tübingen, Wilhelmstrasse 56, D-72074 Tübingen, Germany

[1] *Current address*: Alfred-Wegener Institut für Polar- und Meeresforschung Am Handelshafen 12, D-27571 Bremerhaven, Germany

Editorial responsibility: J. Hoefs

Introduction

The European Volcanic Province (EVP) comprises predominantly alkali basalts of Tertiary to Quaternary age that occur in the Massif Central in France, central Germany (e.g. Eifel, Hesse), lower Silesia in Southwest Poland, and the Pannonian Basin in Hungary. The Urach and Hegau volcanic fields in southern Germany are unique in that only small volume melts such as olivine melilitites were erupted (Fig. 1). The major volcanic centres in central Europe are confined to regions of uplifted Hercynian basement and rifts that were formed during the collision of the African and European plates (Wimmenauer 1974; Ziegler 1992).

The trace element and isotopic composition of the majority of primitive basalts in the EVP suggest sources similar to those of ocean island basalts (OIB) belonging to the HIMU-type family (Wörner et al. 1986; Blusztajn and Hart 1989; Schleicher et al. 1991; Wilson and Downes 1991; Walter et al. 1994; Wilson et al. 1995). An ongoing debate is concerned with the origin of the HIMU mantle source and the effects of melt interaction with the lithosphere. In the course of the investigations a variety of genetic scenarios have been proposed such as melting of the asthenosphere due to lithospheric flexuring, melting of enriched lower

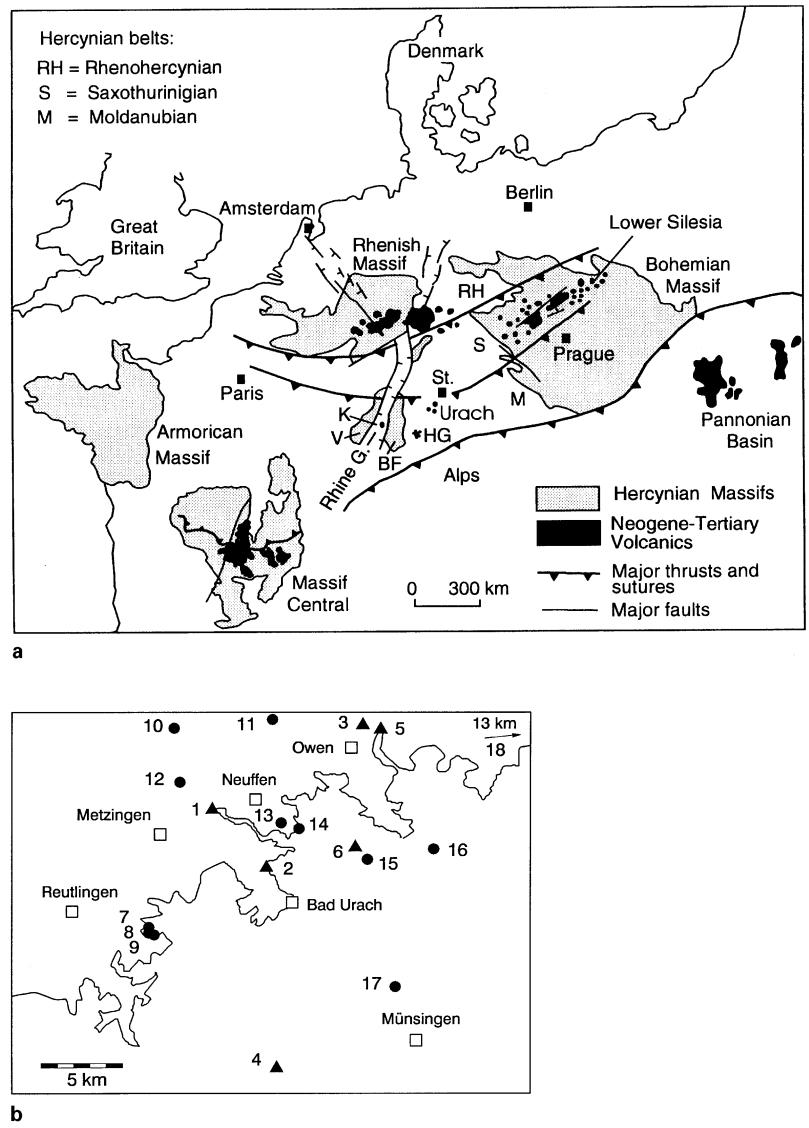

Fig. 1a Map of the Tertiary European Volcanic Province modified after Wimmenauer (1974) and Ziegler (1992). The Urach, Hegau (*HG*), and Kaiserstuhl (*K*) volcanic fields are shown in southern Germany. The major areas of volcanism in Eifel, Hesse (Germany), Massif Central (France), and lower Silesia (SW Poland) are outlined. (*St* Town of Stuttgart, *BF* Black Forest Mts., *V* Vosges Mts. **b** Map of the Bad Urach volcanic field showing the sample locations. The ragged line shows the escarpment of the Jurassic Alb plateau. *Triangles* represent melilitite localities, *solid circles* show tuffaceous diatremes with megacrysts. Sample locations: *1* Jusi, *2* Buckleter Kapf, *3* Götzenbrühl, *4* Sternberg, *5* Hohenbol, *6* Grabenstetten, *7* Bürzlen, *8* Drackensberg, *9* Petersteich, *10* Kräuterbuckel, *11* Kräuterbühl, *12* Grafenberg, *13* Grendenbach, *14* Neuffener Steige, *15* Biegel, *16* Donntal, *17* Hofbrunnen, *18* Burren

lithosphere, melting of subducted Hercynian oceanic lithosphere, and melting of small mantle diapirs. The chemical diversity in mantle xenoliths suggests that subduction processes and terrane accretion during the Hercynian orogeny may have produced substantial heterogeneities in the lithospheric mantle under central Europe. It is reasonable to assume that melting of metasomatized lithospheric mantle with unique histories and mixing of asthenospheric and lithospheric melts may account for the wide chemical spectrum in basalt compositions.

In this paper we present chemical and isotopic data for olivine melilitites and comagmatic clinopyroxene, hornblende, and phlogopite megacrysts from the Urach volcanic field in southern Germany. Melilitites represent incipient, small melt fractions of the mantle and it can be assumed that their composition reflect the characteristics of domains enriched in volatiles and incompatible elements that are melted at a lower temperature than depleted mantle peridotite (e.g. Davies 1984). We suggest that the Urach megacryst and melilitite data can be used to constrain the composition of the ubiquitous OIB-like mantle source of the Tertiary European volcanics.

Geological and geochemical background

The Urach volcanic field is located in the Moldanubian zone of the Hercynian orogen in southern Germany (Fig. 1). At the town of Bad Urach about 30 km south of Stuttgart an area of about 40×50 km shows about 350 tuffaceous diatremes and 16 olivine melilitite occurrences. The volcanic centres are located within a geological trough interpreted to reflect an older basement structure (Glahn et al. 1992). Paleontological evidence (Von Engelhardt and Weiskirchner 1963) and

K-Ar dating (Lippolt et al. 1973) indicate volcanic activity at about 16 to 17 Ma.

Seismic and petrologic investigations of the lithosphere under the Urach volcanic field have been undertaken by Sachs (1988), Mengel et al. (1991), and Glahn et al. (1992). Crustal xenoliths comprise two predominant types: high-grade metasediments (cordierite-biotite gneisses, sillimanite-cordierite gneisses) form the upper and middle crust and metacumulates (pyroxenites, hornblendites, clinopyroxene-mica schists) from the lower crust. The basement is overlain by Upper Jurassic limestones of the Swabian Alb.

Abundant spinel-phlogopite wehrlites and spinel wehrlites reflect pervasive metasomatism of the lithospheric mantle below the Urach volcanic field. A distinct velocity reduction in the upper 50 km of the lithospheric mantle has been correlated with highly metasomatized mantle rocks. In contrast, in the Tertiary Hegau volcanic field, located about 70 km to the southwest, spinel harzburgites and rare spinel websterite suggest a highly depleted lithospheric mantle composition. Petrological and seismic data indicate spinel-garnet phase transition at about 70 to 80 km depth and a lithosphere-asthenosphere transition zone at about 90 km. Deformational features in the xenoliths and exsolution of clinopyroxene support a model of an uplifting lithospheric mantle. The uplift has been attributed to melt-induced density instabilities at the base of the lithosphere and upwelling of the asthenosphere (Glahn et al. 1992).

Melting experiments suggest an origin of the Urach melilitites by $<5\%$ equilibrium partial melting of garnet lherzolite at about 30 kbar and in the presence of H_2O and CO_2 (Brey and Green 1975, 1976, 1977). Alibert et al. (1983) argued for melting degrees as low as 0.2% on the basis of highly incompatible element concentrations. Published major element analyses for the melilitites indicate extreme undersaturation in SiO_2, high $MgO + CaO$, and low Al_2O_3/CaO (Brey 1978; Alibert et al. 1983). Very high Mg-values of 75 to 80 are consistent with accumulation of olivine xenocrysts. The ε_{Nd} values for eight whole-rock samples range from $+2.6$ to $+5.3$ and $^{87}Sr/^{86}Sr$ ratios from 0.7036 to values as high as 0.7043 (Alibert et al. 1983; Wörner et al. 1986; Walter et al. 1994; Wilson et al. 1995).

Samples

Twenty-two pristine clinopyroxene, hornblende, and phlogopite megacryst samples, separated from tuffaceous melilitites collected at twelve diatremes were prepared for isotopic analyses. Two samples of Cr-diopside xenocrysts, from spinel lherzolite xenoliths, were also analysed. We included four samples of an altered phlogopite megacryst variety that apparently is not comagmatic with the melilitites. Sample localities are given in Tables 1 and 2 and shown in Fig. 1b. Electron microprobe analyses of the clinopyroxene megacrysts indicate compositions ranging from Ti-augite to diopside-salite. The hornblende megacrysts are homogeneous and of pargasitic composition. Pristine bronze- will be coloured mica and a greenish chloritized variety may be classified as phlogopites on the basis of Mg values [$Mg\# = Mg/(Mg + Fe^+)$] between 81 and 87. K_2O can be as low as 0.2 wt.% in the greenish altered variety versus 9 to 9.9 wt% in the fresh megacrysts. The CaO concentrations are about 1.5 to 2 wt% in the altered grains and below detection limit in the fresh phlogopites. The electron microprobe data of the minerals are available on request.

Seven melilitite whole-rock samples from six localities were selected from a large collection of Urach melilitites at the University of Tübingen. Although the samples represent the freshest specimens, they show typical small crosscutting calcitic veins suggesting that their Sr isotopic composition may not be primary. Inspection of thin sections shows olivine and clinopyroxene phenocrysts (Ti-augite or diopside-salite), and olivine xenocrysts, set in a groundmass of melilite and clinopyroxene, with perovskite and magnetite as accessory minerals.

Sample preparation and analytical methods

Hornblende, clinopyroxene, and Cr-diopside ranging in size from 1 to 10 mm were picked under a binocular and washed in 2N HCl to remove calcite from the tuff matrix. The mineral separates were crushed in an agate mortar and pristine grains were picked under a binocular from a 0.5 to 0.3 mm sieve fraction. The samples were then washed again in an ultrasonic bath in 2N HCl and rinsed in ultra-pure water. The phlogopite megacrysts were washed in 0.5N HCl for ten minutes and two minutes in 2N HCl. Pristine grains were picked under a binocular from a 0.3 to 0.5 mm sieve fraction. The whole-rock samples were crushed in a jaw crusher and about 50 g of hand-picked optically fresh rock chips were ground in an agate mill.

The Sr isotopic compositions of the melilitites were determined on whole-rock powders leached for 3 hours in 2 N HCl at 80° C and on untreated rock powders. The Sm-Nd isotopic measurements were performed on unleached sample powders. Lead isotopic analyses were performed on whole-rock powders and on untreated rock chips for data comparison. We did not analyse the Pb isotopic compositions of HCl-leached rock chips because our test results showed that this procedure resulted in removal of an unradiogenic Pb component, probably from altered melilite. For Pb isotopic analyses clinopyroxene and hornblende samples were boiled in 6N HCl for one hour, leached for ten minutes in a mixture of 5% HF and 0.8N HBr, and washed in ultra-pure water before decomposition. Phlogopite samples were washed three times for about 15 minutes in 0.8N HBr and rinsed in ultra-pure water before decomposition.

The samples were spiked with mixed ^{84}Sr-^{87}Rb, ^{150}Nd-^{149}Sm, and ^{208}Pb tracers and dissolved in HF-$HClO_4$ for Nd and Sr isotopic analyses, and HF-HNO_3 for Pb isotopic analyses. Rb, Sr, and the LREE were separated on quartz columns with a 5 ml resin bed of AG 50W-X12, 200–400 mesh. Nd was separated from Sm on quartz columns using 1.7 ml Teflon powder coated with HDEHP as cation exchange medium. Pb was separated on Teflon columns containing 80 µl AG 1-X8, 100–200 mesh and employing a HBr-HCl wash and elution procedure. Other details of the analytical procedures are given in Hegner et al. (1995). The Sm-Nd and Rb-Sr isotopic analyses of the USGS basalt standard BCR-1 yielded ($n = 12$): Rb = 46.8 ppm $\pm$0.5%, Sr = 330.7 $\pm$0.06%, Sm = 6.56 ppm $\pm$0.08%, and Nd 28.69 $\pm$0.09%, $^{147}Sm/^{144}Nd = 0.1383 \pm 0.03\%$, $^{143}Nd/^{144}Nd = 0.512629 \pm 2$ (1SD). Four analyses of SRM 607 yielded: Rb = 525 ppm $\pm$0.17%, Sr = 65.9 $\pm$0.15%, $^{87}Rb/^{86}Sr = 24.16 \pm 0.04$, $^{87}Sr/^{86}Sr = 1.20095 \pm 2$. Total procedure blanks during this study were: Sr $<$ 200 pg, Nd, Sm $<$ 30 pg, and Pb 20 to 60 pg.

The isotopic measurements were made in static collection mode on a Finnigan MAT 262 mass spectrometer. Strontium was loaded

Table 1 Major and trace element concentrations for Urach melilitites. Major element concentrations in wt%, trace element concentrations in ppm (*LOI* loss on ignition)

Sample locality	1 Jusi	2 Buckleter Kapf	3 Götzenbrühl	4 Sternberg	5 Sternberg	6 Hohenbol	7 Grabenstetten
SiO_2	35.03	34.02	37.22	34.90	35.90	36.15	34.22
TiO_2	2.38	2.17	2.45	2.77	2.64	2.22	2.77
Al_2O_3	8.20	7.57	8.54	6.73	7.68	7.93	8.42
Fe_2O_3[a]	10.96	10.70	10.48	11.69	11.03	10.44	10.63
MnO	0.20	0.19	0.18	0.19	0.19	0.19	0.19
MgO	16.21	18.16	18.24	20.41	19.63	19.35	15.89
CaO	17.56	17.77	14.89	15.60	15.02	15.71	17.83
Na_2O	0.86	1.50	2.56	1.17	2.55	1.95	1.97
K_2O	0.87	0.28	1.89	0.54	1.76	1.29	1.44
P_2O_5	0.89	0.98	0.76	0.73	0.77	0.82	1.15
L0I	5.31	5.03	0.92	4.05	0.80	2.09	2.71
Sum	98.47	98.37	98.13	98.78	97.97	98.14	97.22
$Mg^{\#}$	77.4	79.8	80.2	80.3	80.6	81.2	77.7
Cr	859	1064	1208	1275	1100	1302	778
Ni	285	365	418	471	460	483	280
Rb	27.1	21.2	65.7	22.7	48	46.2	50.2
Sr	1024	1076	924	876	933	1067	1160
Y	18.5	17.7	17.1	14.6	20	17.2	18.5
Zr	271	239	221	222	268	206	255
Hf	5.79	5.30	5.03	4.71		4.21	6.00
Nb	102	143	106	113	111	100	138
Ba	1004	1141	1068	633	950	1029	1123
La	77.5	99.4	74.8	82.6		81.7	103
Ce	152	181	142	161		154	189
Pr	16.7	18.6	15.3	17.6		16.6	20.1
Nd	62.8	66.2	54.5	65.1		59.6	72.5
Sm	10.3	10.7	8.9	10.3		9.6	11.9
Eu	2.86	3.04	2.83	3.00		3.12	3.56
Tb	0.87	0.86	0.95	1.00		0.99	1.19
Dy	4.65	4.58	3.99	4.08		4.40	5.04
Ho	0.77	0.75	0.73	0.63		0.72	0.83
Er	1.79	1.84	1.77	1.37		1.75	1.82
Tm	0.24	0.23	0.22	0.16		0.23	0.21
Yb	1.51	1.33	1.27	0.94		1.44	1.34
Lu	0.21	0.20	0.19	0.11		0.18	0.19
Pb	3.53	4.66	4.87	2.44		4.56	4.75
Th	10.1	15.8	10.6	11.4		11.4	13.9
U	2.80	4.13	2.59	2.26		2.67	3.15
K/Na	1.0	0.19	0.74	0.46	0.69	0.66	0.73
P/Nd	62	65	61	50	58	60	69
Sr/Nd	16.0	15.0	15.8	12.7	15.6	16.7	15.1
Nb/Th	10.1	9.1	10.0	9.9		8.8	9.9
Ba/Th	100	72	101	56		93	74
La/Nb	0.76	0.70	0.71	0.73		0.82	0.75
Ba/Nb	9.8	7.8	10	5.6	8.6	10	8.1
Zr/Hf	47	45	44	47		49	43
Th/U	3.6	3.8	4.1	5.0		4.3	4.4
Nb/U	36	35	41	50		37	44
Ce/Pb	43	39	29	66		34	40

[a] Total iron listed as Fe_20_3, Mg# is based on $Fe_2O_3/FeO = 0.15$

with a Ta-HF activator and measured on a single W filament. Rb (loaded as chloride) and Sm, Nd (loaded as phosphates) were measured in a Re double filament configuration. Pb was loaded with Si-Gel-H_3PO_4 and measured on a single Re filament at 1300° C.

$^{87}Sr/^{86}Sr$ ratios are normalized to $^{86}Sr/^{88}Sr = 0.1194$, $^{143}Nd/^{144}Nd$ to $^{146}Nd/^{144}Nd = 0.7219$, and Sm isotopic ratios to $^{147}Sm/^{152}Nd = 0.56081$. Measurements of the La Jolla Nd standard yielded $^{143}Nd/^{144}Nd = 0.511851 \pm 12$ (2 SD; $n = 12$), and the NBS 987 Sr standard gave a $^{87}Sr/^{86}Sr$ of 0.710217 ± 24 (2 SD $n = 25$). Rb isotopic ratios are corrected for 0.3% fractionation per mass unit. Twenty analyses of NBS SRM 981 gave $^{206}Pb/^{204}Pb = 16.935 \pm 9$, $^{207}Pb/^{204}Pb = 15.486 \pm 12$, and $^{208}Pb/^{204}Pb = 36.689 \pm 35$ (2 SD). The ratios are corrected for 0.1% fractionation per mass unit, and have an estimated accuracy of 0.03% (2 SD) per mass unit.

Table 2 Sr and Nd isotopic data for megacrysts and melilitites. Concentrations in ppm. External precision: $^{143}Nd/^{144}Nd = 1.2 \times 10^{-5}$, $^{89}Sr/^{86}Sr = 2.4 \times 10^{-5}$, (hornblende) corrected for 16 Ma-(*phl com* comagmatic phlogapites, *phl-xc* phlogapites of crystal origin, *cpx* clinopyroxene, hbl

Locality	Sample	Sm	Nd	$^{147}Sm/^{144}Nd$	$^{143}Nd/^{144}Nd$	ε_{Nd}	Rb	Sr	$^{87}Rb/^{86}Sr$	$^{87}Sr/^{86}Sr$
Grendenbach	Cpx	2.70	10.32	0.1581	0.512864	4.4	0.057	103	0.0016	0.703453
	Phl xc				0.512241	− 7.7	187	6.2	87.3	0.705800
	Hbl	4.76	19.30	0.1493	0.512863	4.4	14.0	273	0.148	0.703464
										0.7034 (t)
Kräuterbuckel	Cpx	4.04	17.67	0.1382	0.512855	4.2	0.39	116	0.0097	0.703474
Grafenberg	Phl xc	0.126	0.648	0.1177	0.512252	− 7.5	15.2	51.4	0.854	0.710338
Drackensberg	Cpx	3.34	14.06	0.1436	0.512800	3.2	0.05	90.9	0.0016	0.703438
	Phl xc	0.626	3.53	0.1073	0.512715	1.5	0.412	11.1	0.107	0.706520
	Hbl	3.95	16.50	0.1447	0.512796	3.1	11.0	376	0.085	0.703474
										0.7035 (t)
Neuffener Steige	Cr-diopside	2.39	11.90	0.1215	0.512824	3.6	0.017	125	0.0004	0.703498
Hofbrunnen	Cpx	2.80	10.87	0.1557	0.512837	3.9	0.113	105	0.0031	0.703470
	Hbl	3.74	15.44	0.1464	0.512846	4.1	12.3	262	0.135	0.703475
										0.7034 (t)
Donntal	Phl com	0.132	0.786	0.1019	0.512805	3.3	336	141	6.91	0.705736
										0.7043 (t)
Burren	Cpx	2.41	8.86	0.1644	0.512897	5.1	0.263	84.5	0.009	0.703319
	Phl xc				0.512240	− 7.8	1.15	8.8	0.379	0.707820
Biegel	Hbl	2.84	11.46	0.1498	0.512882	4.8	11.0	181	0.175	0.703354
										0.7033 (t)
Kräuterbühl	Cr-diopside	2.24	10.40	0.1302	0.512863	4.4	0.654	99.4	0.019	0.703488
Petersteich	Cpx	2.20	8.46	0.1574	0.512775	2.7	0.030	86.7	0.001	0.703418
	Hbl	3.76	15.76	0.1446	0.512819	3.5	10.5	359	0.085	0.703458
Bürzlen	Cpx	2.68	10.52	0.1540	0.512803	3.2	0.077	93.3	0.002	0.703453
	Phl xc	0.0365	0.188	0.1168	0.512722	1.6	48.4	30.1	4.66	0.705340
	Phl com						305	113.7	7.76	0.705252
										0.7035 (t)
	Hbl	5.17	22.32	0.1400	0.512811	3.4	11.9	431	0.08	0.703442
Jusi	Melilitite (#1)	10.4	63.92	0.09855	0.512824	3.6	27.1	1024	0.0765	0.703734
										0.703607[a]
Buckleter Kapf	Melilitite (#2)	11.1	71.54	0.09415	0.512843	4.0	21.2	1076	0.0569	0.703824
										0.703600[a]
Götzenbrühl	Melilitite (#3)	9.50	58.64	0.09800	0.512833	3.8	65.7	924	0.205	0.703636
										0.703610[a]
Sternberg	Melilitite (#4)	11.0	68.89	0.09688	0.512855	4.2	22.7	876	0.0748	0.703393
										0.703412[a]
Sternberg	Melilitite (#5)	9.74	59.80	0.09855	0.512866	4.4	48.0	933	0.149	0.703445
										0.703464[a]
Hohenbol	Melilitite (#6)	10.1	63.94	0.09588	0.512825	3.6	46.2	1067	0.125	0.703780
										0.703601[a]
Grabenstetten	Melilitite (#7)	12.4	76.62	0.09744	0.512848	4.1	50.2	1160	0.125	0.703689
										0.703635[a]

[a] Measured on acid-leached sample powders

Major and some trace elements (Cr, Ni, Zr, Nb) were analysed by XRF. Other trace element concentrations including the rare earth elements (REE) were determined by ICP-MS (inductively coupled plasma-mass spectrometry). Typical values for precision and accuracy of the ICP-MS data are given in Jenner et al. (1990). The Sm, Nd, Rb, Sr, and Pb concentrations of the megacryst samples were determined by isotope dilution.

Results

Major and trace element concentrations of olivine melilitites

Major and trace element concentrations of seven olivine melilitites are listed in Table 1. The melilitites are characterized by low SiO_2 concentrations (34–37%), low Al_2O_3 concentrations (6.7–8.5%), and high CaO concentrations (14.9–17.8%). The MgO concentrations of 15.9 to 20.4% (Mg# 74–79) are very high due to the presence of olivine xenocrysts. The Urach melilitites are compositionally similar to those from the Hegau volcanic field about 70 km to the west (Keller et al. 1990). Olivine accumulation and fractionation can explain the major element variations whereas clinopyroxene fractionation appears not to be important as suggested by the similar CaO/Al_2O_3 ratios of the samples. A positive correlation of the Cr concentrations with MgO and Ni can be explained by inclusions of Cr-spinel in olivine (Ralf Milke, Tübingen; personal communication).

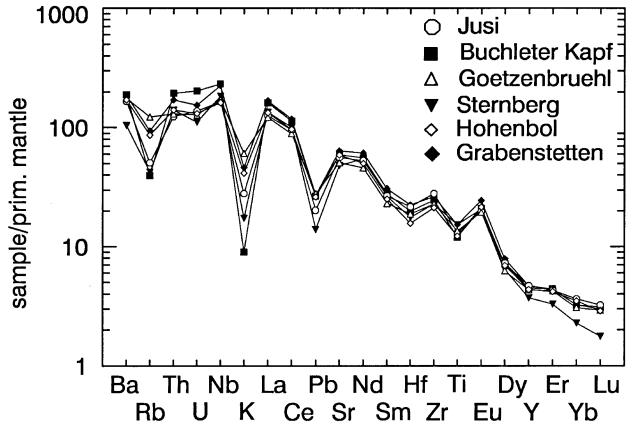

Fig. 2 Primitive mantle-normalized trace element concentrations for six olivine melilitites. The sequence of element incompatibility and normalizing values are from Hofmann (1986)

The incompatible trace element distribution patterns for six melilitites are very similar (Fig. 2). They are characterized by increasing enrichment from Lu to La, with a maximum enrichment for Nb, and decreasing concentrations for the highly incompatible elements U, Th, and Ba. The extended REE patterns display negative anomalies for Rb, K, Pb, and Ti. The element distribution patterns are similar to those of HIMU-type ocean island basalts (Weaver 1991a, b) except that Urach melilitites are more depleted in the HREE concentrations (e.g. Lu is about 1 to 3 times primitive mantle) and more enriched in the highly incompatible elements (up to 200 times relative to primitive mantle values).

$^{87}Sr/^{86}Sr$ and $^{143}Nd/^{144}Nd$ isotopic data

$^{87}Sr/^{86}Sr$ and $^{143}Nd/^{144}Nd$ isotopic ratios for twenty-two augite, Cr-diopside, hornblende, and phlogopite megacryst samples, and seven olivine melilitite whole-rock samples are listed in Table 2. Also listed are the Sr isotopic data obtained on acid-leached whole-rock powders. The isotopic data are plotted in Fig. 3 a and b.

Augite and hornblende megacrysts

The measured $^{143}Nd/^{144}Nd$ and $^{87}Sr/^{86}Sr$ ratios for thirteen augite and hornblende samples range from 0.51278 to 0.51290 (ε_{Nd} +2.6 to +5.1) and 0.7033 to 0.7035, respectively (Fig. 3a). The Rb/Sr and Sm/Nd ratios of these samples are very low so that in-situ decay over 16 Ma for most samples lies within the analytical error of the measured ratios (see Table 2). Except for two samples, the augite and hornblende megacryst samples have very similar $^{87}Sr/^{86}Sr$ ratios

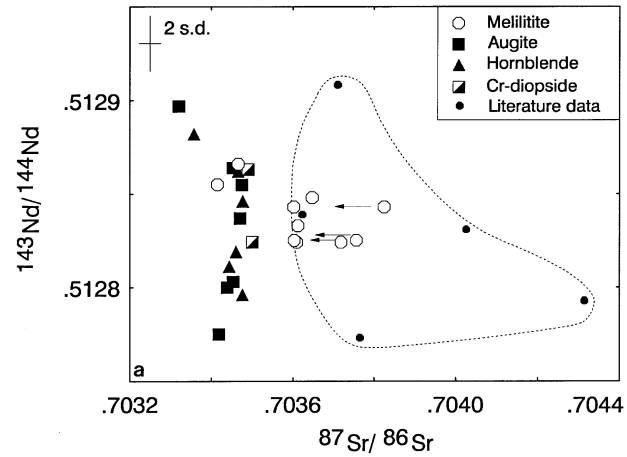

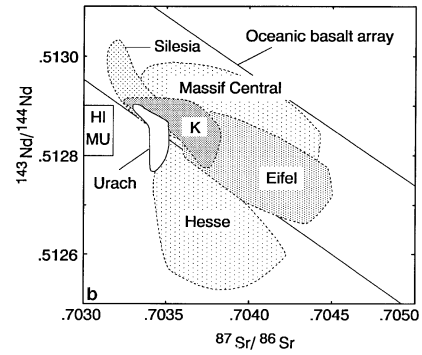

Fig. 3a $^{87}Sr/^{86}Sr$ and $^{143}Nd/^{144}Nd$ ratios for melilitites, augite, hornblende, and Cr-diopside samples. The *arrows* indicate whole-rock compositions after acid leaching; the data points *outlined* are considered suspicious. The phlogopite megacryst data are not shown. They define two groups: samples with $^{143}Nd/^{144}Nd$ ratios similar to the whole rocks, and a second group with very low $^{143}Nd/^{144}Nd$ of about 0.5122 (Table 1). Published data are shown for comparison (Alibert et al. 1983; Wörner et al. 1986). **b** The Urach data in comparison with Tertiary volcanics from central Europe. Data sources: Alibert et al. 1983; Massif Central (Downes 1984; Chauvel and Jahn 1984; Briot et al. 1991), Eifel and Hesse (Kramers et al. 1981; Wörner et al. 1986; Kramm and Wedepohl 1990; Wedepohl et al. 1994), Kaiserstuhl (*K*; Nelson et al. 1988; Wedepohl et al. 1994), and Silesia (Alibert et al. 1987; Blusztajn and Hart 1989). HIMU mantle component after Zindler and Hart (1986)

but show a significant variation in $^{143}Nd/^{144}Nd$ ratios which results in a distinct vertical data trend.

Phlogopite megacrysts

The $^{143}Nd/^{144}Nd$ ratios for six phlogopite samples indicate an origin from two distinct sources. These can be assigned to the melilititic melts and the lower crust. Phlogopite megacrysts comagmatic with the melilitites occur at Donntal and Bürzlen. The Nd isotopic composition of the Donntal sample is similar to the value of the melilitites, augite, and hornblende megacrysts ($\varepsilon_{Nd} \cong +3.3$; Table 2; for the Bürzlen sample only Sr

and Pb isotopic data are available). The calculated initial Sr isotopic ratio for the Donntal sample has a very high value of 0.7043 when compared to the low value of 0.7035 for Bürzlen phlogopite sample. We interpret the high value as reflecting disturbance of the Rb-Sr isotopic system. For example an age estimate for the Donntal phlogopite in combination with the pyroxene analyses that best reflect the range in inital Sr ratios of the Urach volcanism values (e.g. $^{87}Sr/^{86}Sr$ of 0.7034–0.7035) suggest crystallization between 23 and 24 Ma. These ages are about 50% higher than the 16 Ma determined for the Urach volcanism (Lippolt et al. 1973). The age discrepancy supports our conclusion that the high age-corrected Sr isotopic ratio of 0.7043 is most likely not primary. Considering the spectrum of different degrees of alteration in the phlogopite samples, we accept their Nd isotopic compositions as more meaningful. Phlogopite megacryst samples of crustal origin occur at five localities. Samples from Drackensberg and Bürzlen have have ε_{Nd} values of about $+1.5$. Although these values are not much different from those for the melilitites and comagmatic megacrysts, Pb isotopes presented below indicate that these samples are not related to the melilitites. Phlogopite samples from Grendenbach, Grafenberg and Burren have very low $^{143}Nd/^{144}Nd$ ratios of about 0.51225 ($\varepsilon_{Nd} \cong -8$). The Sm/Nd ratios in these samples are similar to those in granitoids and therefore their isotopic evolution mimics a crustal trend. The measured Nd isotopic compositions of these phlogopites and their Nd model ages are similar to those of the most enriched Variscan granites from the Black Forest, Vosges, and Odenwald (Liew and Hofmann 1988; Langer et al., in preparation) and we interpret them to reflect the composition of the lower crust under the Urach volcanic field.

Olivine melilitites

The $^{143}Nd/^{144}Nd$ and $^{87}Sr/^{86}Sr$ ratios for seven melilitites of this study and five samples from the literature (Alibert et al. 1983; Wörner et al. 1986) are plotted in Fig. 3a. The $^{143}Nd/^{144}Nd$ ratios overlap the range displayed by the comagmatic megacrysts but $^{87}Sr/^{86}Sr$ ratios are in most whole-rock samples considerably higher than those in the pyroxene and hornblende megacrysts. The Sr isotopic ratios measured on acid-leached powders are in four samples significantly lower and indicate presence of secondary Sr. These results documents that even at high Sr concentrations, in the Urach melilitites up to 1300 ppm, Sr isotopes may be susceptible to alteration. Based on this observation, it is clear that the Sr isotopic compositions of the whole rocks and the acid-leached powders, must be interpreted as maximum values.

Figure 3b shows the Urach data in comparison with the compositions for other Tertiary volcanics from the EVP. The Urach megacryst samples have among the lowest $^{87}Sr/^{86}Sr$ ratios for the given $^{143}Nd/^{144}Nd$ ratios and plot close to the HIMU mantle component of Zindler and Hart (1986). Tertiary basalts from the Eifel and the Massif Central are more heterogeneous and in particular samples from the Massif Central have more radiogenic Sr isotopic compositions for a given $^{143}Nd/^{144}Nd$ ratio than the Urach samples. Many volcanics from Hesse are distinct in that they plot below the MORB-OIB data array. The most depleted sources of all volcanics are reflected in some basalts from Lower Silesia overlapping the compositions for the most enriched mid-ocean ridge basalts (MORB; White and Hofmann 1982).

Cr-diopside megacrysts

The Nd and Sr isotopic compositions for two Cr-diopside megacryst samples originating from spinel-lherzolite nodules are indistinguishable from those of hornblende, clinopyroxene, and melilitites (Table 2, Fig. 3a). Their $^{147}Sm/^{144}Nd$ ratios of about 0.13 indicate enrichment in LREE, which is in contrast to the Nd isotopic evidence for a long-term isotopic evolution with LREE depletion. Thus the LREE enrichment may be attributed to chemical overprinting of lithospheric mantle by migrating melts during Tertiary volcanism.

Pb isotopic compositions

Olivine melilitites, augite, and hornblende megacrysts

The U-Th-Pb isotopic compositions of the melilitites and the Pb isotopic compositions of the megacryst samples, and their leachates are listed in Tables 3 and 4. The initial ratios for the melilitites are plotted with the measured ratios for the megacrysts in Fig. 4. We have not determined the U and Th concentrations in the megacrysts because partition coefficients for clinopyroxene and phlogopite in alkaline magmas indicate very low Th/Pb ratios and by inference low U/Pb ratios (Foley et al. 1994) so that the measured ratios are probably similar to the initial ratios, and may be compared with the age-corrected whole-rock data. The very radiogenic $^{206}Pb/^{204}Pb$ ratios of 19.37 to 19.85 (Fig. 4a) and moderately radiogenic $^{207}Pb/^{204}Pb$ ratios plot about a reference line for the northern hemisphere mantle composition (NHRL; Hart 1984) in agreement with an OIB source that has evolved with a high U/Pb ratio. In a $^{206}Pb/^{204}Pb$- $^{208}Pb/^{204}Pb$ diagram the data points plot slightly above the NHRL, except for the composition of one augite sample, indicating a source with a slightly higher Th/U than in the reference mantle.

In Fig. 4b the Urach Pb isotopic data are compared with those for volcanics from the Kaiserstuhl in

Table 3 Pb isotopic compositions for melilitites. Pb, U, and Th concentrations are in ppm, $\mu = {}^{238}u/{}^{204}Pb$; $\omega = {}^{232}Th/{}^{204}Pb$; $\kappa = {}^{232}Th/{}^{238}U$; values in parentheses are inferred. Uncertainties are $2\sigma_{mean}$ within-run precision and refer to the last digits. Differences between powder and chips may reflect chip heterogeneity

Sample		Pb	U	Th	$^{206}Pb/^{204}Pb$	$^{207}Pb/^{204}Pb$	$^{208}Pb/^{204}Pb$	μ	ω	κ
1	Powder	3.53	2.80	10.1	19.493 ± 2	15.621 ± 2	39.543 ± 5	51.9	193	3.73
	[a]				19.37	15.61	39.40			
	Rock chips				19.515 ±3	15.622 ±2	39.590 ±6			
2	Powder	4.66	4.13	15.8	19.511 ±1	15.612 ±1	39.446 ±3	57.9	228	3.95
	[a]				19.38	15.61	39.28			
	Rock chips				19.496 ±1	15.601 ±1	39.429 ±3			
3	Powder	4.87	2.59	10.6	19.512 ±2	15.617 ±2	39.494 ±4	34.8	147	4.23
	[a]				19.43	15.61	39.38			
	Rock chips				19.505 ±1	15.615 ±1	39.501 ±2			
4	Powder	2.44	2.26	11.4	19.704 ±3	15.616 ±3	39.631 ±7	60.8	317	5.21
	[a]				19.56	15.61	39.40			
	Rock chips				19.694 ±3	15.622 ±2	39.627 ±5			
5	Powder				19.817 ±5	15.633 ±4	39.744 ±9	(35	150	4.2)[b]
	[a]				19.74	15.63	39.63			
	Rock chips				19.873 ±5	15.640 ±4	39.803 ±9			
6	Powder	4.56	2.67	11.4	19.494 ±3	15.605 ±2	39.478 ±5	38.2	168	4.41
	[a]				19.41	15.60	39.35			
	Rock chips				19.520 ±2	15.616 ±2	39.545 ±5			
7	Powder	4.75	3.15	13.9	19.569 ±1	15.615 ±1	39.517 ±3	43.4	198	4.56
	[a]				19.47	15.61	39.37			
	Rock chips				19.573 ±1	15.614 ±1	39.549 ±2			

[a] Corrected for an age of 16 Ma
[b] Values are estimated

Table 4 Pb isotopic compositions for megacrysts. Pb concentrations are in ppm, uncertainties are $2\sigma_{mean}$ within-run precision and refer to the last digits. (*cpx* clinopyroxene, *hbl* hornblende, *phl com* comagmatic phlogopites megacrysts, *phl xc* phlogopites of crustal origin

Locality	Sample	Pb	$^{206}Pb/^{204}Pb$	$^{207}Pb/^{204}Pb$	$^{208}Pb/^{204}Pb$
Grendenbach	Cpx		19.850 ±10	15.624 ±8	39.541 ±20
	Leachate		18.790 ±16	15.609 ±16	38.644 ±37
Grafenberg	Phl xc	1.42	18.140 ±1	15.572 ±1	38.032 ±2
	Leachate		17.963 ±1	15.580 ±1	37.904 ±2
Drackensberg	Phl xc		17.761 ±15	15.558 ±14	37.613 ±32
	1. Leachate		17.511 ±3	15.528 ±2	37.329 ±6
	2. Leachate		17.509 ±7	15.534 ±6	37.343 ±15
	3. Leachate		17.514 ±14	15.539 ±13	37.351 ±30
	Hbl	0.200	19.757 ±8	15.627 ±7	39.616 ±17
Hofbrunnen	Hbl		19.450 ±6	15.619 ±5	39.378 ±13
Donntal	Phl com		19.573 ±5	15.615 ±4	39.470 ±10
	Leachate		18.319 ±7	15.583 ±5	38.178 ±15
Burren	Brown cpx	0.048	19.420 ±20	15.617 ±16	39.288 ±41
	Leachate		17.809 ±21	15.565 ±17	37.584 ±45
	Green cpx	0.129	19.592 ±7	15.615 ±5	39.474 ±14
	Phl xc		18.256 ±4	15.586 ±4	38.030 ±9
	1. Leachate		17.737 ±2	15.553 ±2	37.585 ±4
	2. Leachate		17.792 ±7	15.559 ±7	37.635 ±15
Biegel	Hbl		19.574 ±4	15.601 ±3	39.410 ±8
Kräuterbühl	Cr-diops (1)	0.322	19.046 ±12	15.602 ±10	39.018 ±25
	Leachate		17.506 ±2	15.524 ±2	37.336 ±4
	Cr-diops (2)		19.168 ±14	15.579 ±11	39.105 ±28
	Leachate		17.564 ±6	15.533 ±6	37.417 ±13
Petersteich	Cpx	0.058	19.620 ±21	15.613 ±17	39.499 ±42
	Leachate		18.019 ±25	15.576 ±22	37.788 ±53
	Hbl		19.714 ±10	15.627 ±8	39.584 ±21
Bürzlen	Cpx	0.049	19.685 ±31	15.638 ±25	39.590 ±63
	Phl xc		18.241 ±6	15.597 ±5	38.146 ±12
	Leachate		18.034 ±5	15.581 ±4	37.908 ±10
	Phl com		19.639 ±6	15.626 ±5	39.510 ±12
	Hbl		19.782 ±6	15.625 ±5	39.643 ±12

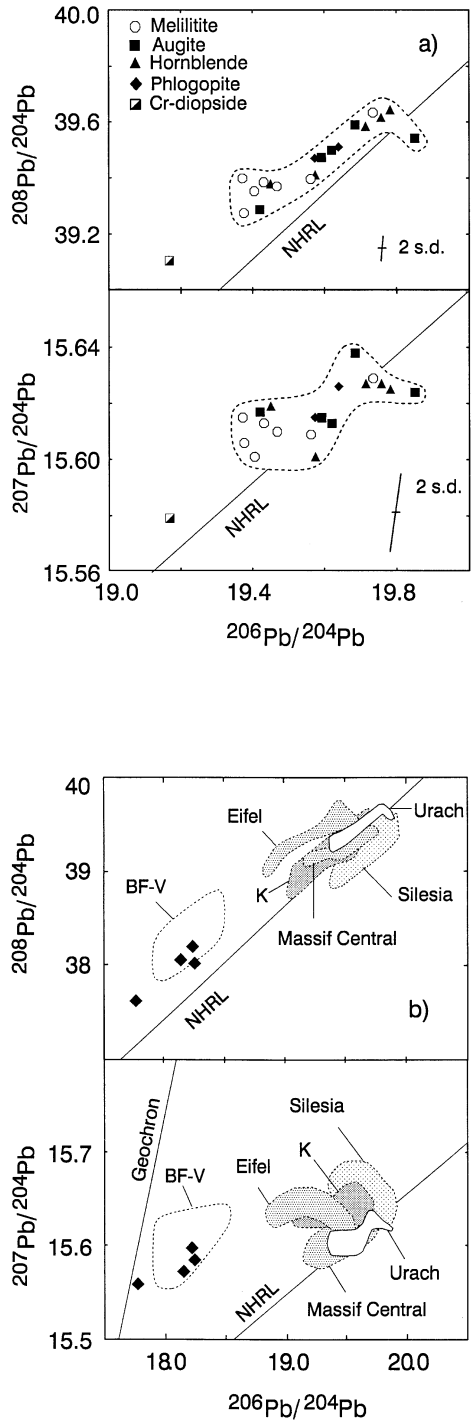

Fig. 4a Pb isotopic compositions for Urach megacrysts (measured ratios) and melilitites (corrected for 16 Ma). *NHRL* represents a reference composition for the northern hemisphere mantle (Hart 1984). **b** Comparison of the Urach data with the composition of Tertiary volcanics from central Europe (Blusztajn and Hart 1989; Nelson et al. 1988; Schleicher et al. 1991; Wörner et al. 1986; Wilson and Downes 1991). Urach samples are distinct in that they have the most radiogenic $^{206}Pb/^{204}Pb$ ratios combined with the lowest $^{207}Pb/^{204}Pb$ ratios precluding a significant contribution from old crust. The *diamonds* represent isotopically unusual phlogopite megacrysts from Urach diatremes that are similar to Hercynian basement from the Vosges (*V*) and Black Forest (*BF*; Vitrac et al. 1981; Vidal and Postaire 1985; Kober and Lippolt 1985)

southern Germany, Eifel, Silesia, and the Massif Central. A striking feature of many EVP basalts is their high $^{207}Pb/^{204}Pb$ ratios that plot predominantly above the NHRL consistent with melting of an old crustal component. It is not clear if the old Pb component in these volcanics was derived from the Hercynian basement or subducted old sediment stored in the lithospheric mantle. Urach melilitites and Silesian alkali basalts have the most radiogenic $^{206}Pb/^{204}Pb$ ratios but typical OIB source characteristics without an old Pb component are only reflected in the Urach samples.

Phlogopite megacrysts

The Pb isotopic compositions of six phlogopite megacryst samples show two different populations that are interpreted as reflecting Tertiary magmatic and old crustal sources, respectively. The $^{206}Pb/^{204}Pb$ and $^{207}Pb/^{204}Pb$ ratios of two pristine megacryst samples from Donntal and Bürzlen plot in a data field for melilitites and augite, hornblende megacrysts (Fig. 4a). These samples can be explained as being comagmatic with the other megacrysts. The other four phlogopite megacryst samples have very low $^{206}Pb/^{204}Pb$ ranging from 17.7 to 18.25 and high $^{207}Pb/^{204}Pb$ of about 15.58 plotting above the NHRL (Fig. 4b). Their compositions are similar to that of Hercynian granitoids from the Black Forest and the Vosges (Vitrac et al. 1981; Kober and Lippolt 1985; Vidal and Postaire 1985) about 80 to 250 km to the west of the study area. We interpret them to reflect the composition of the Hercynian lower crust beneath the Urach volcanic field as supported by very low ε_{Nd} values of about -8 in three samples (Table 2). Phlogopite samples from Drackensberg and Bürzlen localities have higher ε_{Nd} values of about $+1.5$ consistent with an origin from Hercynian lower crust containing a significant juvenile component. The combination of a typical crustal Pb and a depleted mantle-like Nd isotopic signature for these samples can be explained by assimilation of small amounts of old felsic crust by a mantle-derived magma. This process would have a significant effect on the Pb isotopic system due to the high Pb concentrations in the crust whereas the Sm-Nd isotopic system would retain the depleted mantle characteristics.

Cr-diopside megacrysts

A single Cr-diopside megacryst sample was analyzed in duplicate for its Pb isotopic composition after leaching for 10 and 20 minutes in dilute HF-HBr. The results are significantly different, with the more strongly leached sample showing a lower $^{207}Pb/^{204}Pb$ and higher $^{206}Pb/^{204}Pb$ of 19.2 plotting within error limits on the NHRL but to the left of the megacryst and whole-rock

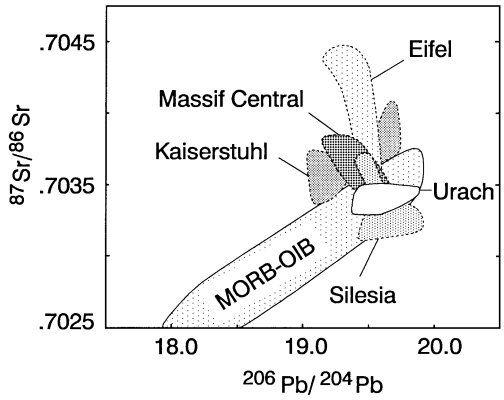

Fig. 5 $^{206}Pb/^{204}Pb$ versus $^{87}Sr/^{86}Sr$ ratios for Urach megacryst samples showing typical OIB characteristics when compared to samples from the Eifel, Massif Central, and Kaiserstuhl. Data sources as in Figs. 3 and 4. MORB-OIB envelope from White (1985)

data. We interpret the data of the more severely leached diopside sample as more meaningful but cannot preclude the possibility of incomplete removal of an unradiogenic Pb component as seen in the leachate. Due to this uncertainty we suggest that the Nd isotopic data for the Cr-diopside samples are more meaningful. As shown in the section on Nd isotopes, the Nd isotopic data of the diopside megacrysts are similar to the compositions of the volcanics, implying a close genetic link that may be explained in terms of melt interaction with depleted lherzolite wall-rock.

$^{87}Sr/^{86}Sr$ and $^{206}Pb/^{204}Pb$ relationship

Figure 5 shows a comparison between the $^{206}Pb/^{204}Pb$ and $^{87}Sr/^{86}Sr$ isotopic compositions of the Urach megacrysts and the data of other volcanics from the EVP. The melilitite whole-rock data are not included because the acid-leaching results show that their Sr isotopic ratios are not reliable. An important observation is the OIB-like composition of the Urach data contrasting with the often higher $^{87}Sr/^{86}Sr$ ratios in volcanics from other regions, except for the Silesian basalts.

Discussion

Composition of low-temperature melting mantle domains

Experimental data and trace element modelling support an origin of melilititic melts by very low degrees of partial melting (e.g. Brey and Green 1977; Alibert et al. 1983). It can be concluded that the formation of melilititic melts will be confined to mantle domains that are enriched in volatiles, heat producing and other highly incompatible elements because of their lower solidus temperature than that of depleted peridotite (e.g. Davies 1984; Sleep 1984). Thus it is reasonable to assume that the Urach melilitite and megacryst data constrain the composition of enriched mantle domains. The involvement of a crustal component can be precluded on the basis of mantle-like Pb isotopic compositions in the melilitites and the absence of mixing trends between the melilitite data points and those of phlogopite xenocrysts of crustal origin (Fig. 4b).

The results of this study indicate that the mantle under the Urach volcanic field comprises mantle domains indistinguishable from the sources of OIB. Some trace element characteristics of the melilitites are similar to those in HIMU-type ocean island basalts. For example the mantle-normalized trace element concentrations in Fig. 2 show a steep REE pattern with the highest enrichment for Nb and decreasing concentrations of highly incompatible elements such as U, Th, Rb, and Ba (Fig. 2). Trace element patterns of this type have been explained with melting of recycled oceanic lithosphere (Hofmann 1988). Negative anomalies for K, Rb, variable Ce/Pb ratios (29 to 66), and low La/Nb ratios (0.7 to 0.8) are consistent with HIMU-OIB source characteristics (Weaver 1991a, b; Chauvel et al. 1992).

Other incompatible trace element ratios listed in Table 1 further support melting of typical OIB sources (McDonough et al. 1985;. Hofmann et al. 1986; Jochum et al. 1986, 1989; Sun and McDonough 1989). For example, Nb/U ratios range from 35 to 50, Nb/Th from 8.8 to 10.1, Ba/Th from 72 to 100 (except sample 4 with a value of 55); Th/U from 3.6 to 5.0, Sr/Nd from 12.7 to 16.7, Zr/Hf from 43 to 49, and P/Nd from 58 to 69 (except for sample no. 4 with a ratio of 50).

The $^{207}Pb/^{204}Pb$ and $^{206}Pb/^{204}Pb$ Pb isotopic ratios of the melilitites plot on a 1.77 Ga secondary isochron for oceanic basalts (NHRL) suggesting that the source rocks of the melilitites have an ancient origin, considerably exceeding that of the Hercynian basement. There is a good agreement with the Pb isotopic compositions of other primitive basalts from the EVP and OIB from the Azores and Canaries (Sun 1980; Hoernle et al. 1991). This observation may be interpreted as evidence for presence of similar low-temperature melting mantle domains on a large scale in the north Atlantic region.

Role of the lithospheric mantle during magma generation

The negative K, Rb, Ti anomalies (Fig. 2) may be explained by fractionation and/or melting in the presence of residual phlogopite, amphibole, and titanate minerals during melt evolution in the lithospheric mantle (e.g. Sun and Hanson 1975; Clague and Frey 1982; Wedepohl 1985; Chauvel and Jahn 1984).

However, Sudo and Tatsumi (1990) reported experimental data showing that phlogopite and potassic amphibole may also be stable at much higher pressures suggesting that negative K and Rb anomalies may not be reliable evidence to preclude melting of sub-lithospheric mantle sources. A number of authors have postulated that melting of metasomatized lithospheric mantle with amphibole and phlogopite will produce ultrapotassic melts (e.g. Foley 1988, and references therein), an inference that is supported by the often unusual radiogenic isotopic compositions for ultrapotassic rocks (e.g. Nelson et al. 1986). It is not clear in this context how the K-deficiency in melilitites with $K_2O/Na_2O < 1$ can be reconciled with models suggesting an origin from lithospheric mantle sources (e.g. Rogers et al. 1992). Polybaric melt fractionation and formation of vein amphibole and phlogopite as has been proposed by Irving (1980) and Irving and Frey (1984) for the origin of alkalic melts may be an alternative process to account for the K-deficiency in some basalts. It is clear that the cause of negative K and Rb anomalies in alkalic basalts remains to be resolved. In this paper we will adopt the conventional interpretation that negative K and Rb anomalies reflect melting conditions in the shallow mantle. This region comprises a thermal boundary layer (tectosphere) and a deeper metasomatized mantle region defined as chemical boundary layer (Jordan 1979).

It has been shown that Ce/Pb ratios in HIMU-type ocean island basalts are often higher and more variable than in MORB and other OIB (Hofmann 1988; Chauvel et al. 1992; Halliday et al. 1988, 1990). Plots of Ce/Pb versus La/Lu, La/K_20, and Ba/Nd ratios (Fig. 6) for the Urach melilitites display well developed data trends (the data point for sample 2 is not plotted in Fig. 6b because of K-loss in this sample). The Ce/Pb ratios in the melilitites decrease from 66 to 29. The lowest value is only slightly higher than those in oceanic basalts, excluding HIMU-type OIB. The decreasing Ce/Pb ratios are accompanied by decreasing La/Lu ratios (Fig. 6a) suggesting that it may be due to variable degrees of partial melting. It can be assumed that fractionation of olivine and pyroxene in the melilitites will not modify the Ce/Pb ratios. In Fig. 6b it can be seen that the Ce/Pb ratios are positively correlated with the degree of K-depletion suggesting a control by residual K-bearing phases such as phlogopite and amphibole. This inference is supported by the data of O'Reilly et al. (1991) and Rosenbaum (1993) showing that amphibole and phlogopite are important hosts for Pb. These phases have also high partitition coefficients for Ba (O'Reilly et al. 1991) which can explain a negative correlation between Ce/Pb and Ba/Nd (Fig. 6c). We conclude that the variable and high Ce/Pb ratios in Urach melilitites and possibly also HIMU-type OIB may reflect residual amphibole and phlogopite during melting of metasomatized mantle rocks.

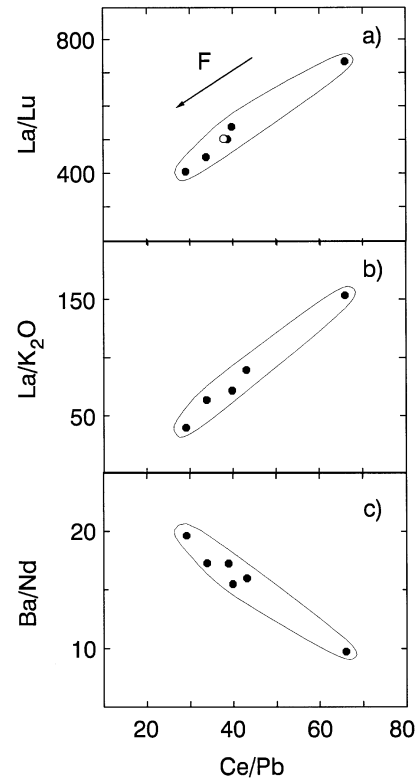

Fig. 6 Variation of Ce/Pb ratios with La/Lu, La/K_2O, and Ba/Nd for Urach melilitites. The data trends are consistent with melting of amphibole and phlogopite in the shallow mantle (see text for discussion). The *arrow* (*F*) indicates increasing melting degrees

It has been argued that metasomatized lithosphere represents an important source for continental basalts (e.g. Menzies and Murthy 1980; Bailey 1982; Hawkesworth et al. 1984, 1990; Menzies et al. 1987; Sun 1989; McKenzie 1989; Foley 1988). The extensive metasomatism of the lithosphere under the Eifel and Hesse located in the Saxothuringian zone of the Hercynian belt (e.g. Lloyd and Bailey 1975; Stosch and Seck 1980; Stosch and Lugmair 1986; Kempton et al. 1988; Witt and Seck 1989; Hartmann and Wedepohl 1990) has been interpreted as an essential precursor for the generation of alkali basalts (e.g. Wilson and Downes 1991; Riley et al. 1994). Extensive metasomatic overprinting of the lithospheric mantle under the Urach volcanic field (Glahn et al. 1992) appears to be closely linked to melting in the asthenopshere as can be inferred from the isotopic data of this study.

The primary source characteristics of Urach volcanism, as provided by the megacrysts data, indicate low $^{87}Sr/^{86}Sr$ ratios combined with variable $^{143}Nd/^{144}Nd$ ratios consistent with a long-term source evolution with a low Rb/Sr ratio and variable depletion in LREE. If the melilitites were generated from a metasomatized lithosphere typically characterized by a high Rb/Sr ratio (McKenzie 1989), it must be concluded that the enrichment cannot have occurred very long before

volcanism. Furthermore, it can be assumed that the metasomatizing melts had a higher U/Pb ratio than those measured in the melilitites. Given a time span of only 50 Ma, the $^{206}Pb/^{204}Pb$ ratio of a model source rock with a U/Pb ratio similar to the lowest value measured in the melilitites ($\mu = 35$ for sample 3, Table 3) would increase by about 0.3. As a consequence, the Pb isotopic composition of a melt from this source would plot to the right of the NHRL because the radiogenic increase in $^{207}Pb/^{204}Pb$ would be negligible. Our interpretation of the isotopic data as evidence for a very young enrichment of the lithospheric mantle under the Urach volcanic field implies that the OIB-like isotopic compositions in Urach melilitites ultimately originate from a sub-lithospheric mantle domain.

Origin of OIB-sources under central Europe

The very heterogeneous Pb isotopic compositions of Tertiary European volcanics (Fig. 4b) indicate involvement of multiple sources. The $^{207}Pb/^{204}Pb$ ratios for Eifel, Kaiserstuhl, and Silesia plot predominantly above the NHRL consistent with assimilation of old basement and melting of subducted old sediment. A similar conclusion can be drawn from the Sr-Pb isotope diagram (Fig. 5) showing that volcanics from the Eifel, Kaiserstuhl and Massif Central have more radiogenic Sr isotopic compositions than in the source of MORB and OIB. An important observation emerging from the Pb-Pb isotope diagram is the fact that the data fields for all volcanic provinces converge on the NHRL at similar $^{206}Pb/^{204}Pb$ ratios as measured for the Urach melilitites. This strongly suggests a common primary source for these rocks indistinguishable from that of OIB. A review of the literature data shows that primitive basalts from the Massif Central, from Silesia, and the Kaiserstuhl with mantle-like Pb isotopic compositions show Nd-Sr isotopic compositions similar to those in the Urach samples supporting our assumption for melting of similar sub-lithospheric sources during Tertiary volcanism.

The origin of the OIB-like mantle component has been explained with a number of models. Wilson and Downes (1991) suggested melting of subducted oceanic lithosphere of Hercynian age, although they did not address the question of how the distribution of oceanic lithosphere can be correlated with former subduction zones. In a more recent study, Wilson et al. (1995) suggested melting of a metasomatized thermal boundary layer as a possible origin of melilitites in western Europe. Wedepohl et al. (1994) proposed a model invoking metasomatized peridotite as the basalt source and a dehydrating oceanic crust as the source of the metasomatizing fluids. Although Tertiary basalts share many of the characteristics of plume-related ocean island basalts, melting of a major plume is not supported by geologic evidence (e.g. uplift of lithosphere). On the other hand melting of small mantle plumes of deep origin is difficult to reconcile with plume dynamics (Griffiths and Campbell 1991; Wilson and Downes 1991). Underplated fossil plumes have been proposed as sources for the Cameroon Line and Sinaii volcanics (Fitton and Dunlop 1985; Stein and Hofmann 1992). In the case of European volcanism this model is not appealing because there is no volcanic or topographic evidence for an ascending large mantle plume in the post Hercynian geologic record.

It has been shown that OIB source rocks are an intrinsic constituent of the asthenosphere possibly due to dispersion of deep mantle plumes (e.g. Schilling 1985; Allegre et al. 1984; Allegre and Turcotte 1986; Galer and O'Nions 1986; White 1993) and delamination of enriched lithospheric mantle (McKenzie and O'Nions 1995). Melting of enriched mantle domains in the shallow asthenosphere can account for the chemistry of seamount basalts with OIB characteristics (e.g. Zindler et al. 1984; Hegner and Tatsumoto 1989). We propose that the chemical characteristics of Tertiary volcanism ultimately originate from melting of enriched OIB-like mantle domains in an upwelling asthenosphere which led to enrichment of the lower lithosphere. Melting of the young chemical boundary layer must have followed closely in time as required by the isotopic data. A distinction between an origin of the postulated OIB source from dispersed deep mantle plumes, derived from subducted oceanic lithosphere (Hofmann and White 1982), or delaminated and metasomatized lithospheric mantle (McKenzie and O'Nions 1995), awaits understanding of element partitioning during metasomatism and the processes that facilitate the preservation of heterogeneities in a convecting mantle.

Acknowledgements G. Brey, A. Glahn, P.M. Sachs, R. Milke, P. Metz, R. Altherr, and his co-workers are thanked for discussions. Thanks are due to U. Neumann for helping us to collect samples, and F. Schumann and G. Bartholomä for the XRF analyses. H. Stosch and G. Witt-Eickschen reviewed a previous version of the manuscript and are thanked for their efforts and helpful suggestions.

References

Allegre CJ, Turcotte DL (1986) Implications of a two-component layer cake mantle. Nature 323:71–84

Allegre CJ, Hamelin B, Dupre B (1984) Statistical analysis of isotopic ratios in MORB:the mantle blob cluster model and the convective regime of the mantle. Earth Planet Sci Lett 71:71–84

Alibert C, Michard A, Albarede F (1983) The transition from alkali basalts to kimberlites:isotope and trace element evidence from melilitites. Contrib Mineral Petrol 82:176–186

Alibert C, Leterrier J, Panasiuk M, Zimmermann JL (1987) Trace and isotope geochemistry of the alkaline Tertiary volcanism in southwest Poland. Lithos 20:311–321

Bailey DK (1982) Mantle metasomatism – continuing chemical change within the Earth. Nature 296:525–530

Blusztajn J, Hart SR (1989) Sr, Nd and Pb isotopic character of Tertiary basalts from southwest Poland. Geochim Cosmochim Acta 53:2689–2696

Brey G (1978) Origin of olivine melilitites – chemical and experimental constraints. J Volcanol Geothermal Res 3:61–88

Brey G, Green DH (1975) The role of CO_2 in the genesis of olivine melilitite. Contrib Mineral Petrol 49:93–103

Brey G, Green DH (1976) Solubility of CO_2 in olivine melilitite at high pressures and the role of CO_2 in Earth's upper mantle. Contrib Mineral Petrol 55:217–23

Brey G, Green DH (1977) Systematic study of liquidus phase relations in olivine melilitite $+H_2O+CO_2$ at high pressures and petrogenesis of an olivine melilitite magma. Contrib Mineral Petrol 61:141–162

Briot D, Cantagrel JM, Dupuy C, Harmon RS (1991) Geochemical evolution in crustal magma reservoirs: trace element and Sr-Nd-O isotopic variations in two continental intra-plate series at Monts Dore, Massif Central, France. Chem Geol 89:281–303

Chauvel C, Jahn BM (1984) Nd-Sr isotope and REE geochemistry of alkali basalts from the Massif Central, France. Geochim Cosmochim Acta 48:93–110

Chauvel C, Hofmann AW, Vidal P (1992) HIMU-EM: the French Polynesian connection. Earth Planet Sci Lett 110:99–119

Clague DA, Frey FA (1982) Petrology and trace element geochemistry of the Honolulu volcanics, Oahu: implications for the oceanic mantle below Hawaii. J Petrol 23:447–504

Davies GF (1984) Geophysical and isotopic constraints on mantle convection: an interim synthesis. J Geophys Res 89:6017–6040

Downes H (1984) Sr and Nd isotope geochemistry of coexisting alkaline magma series, Cantal, Massif Central, France. Earth Planet Sci Lett 69:321–334

Fitton JG, Dunlop HM (1985) The Cameroon Line, West Africa, and its bearing on the origin of oceanic and continental alkali basalts. Earth Planet Sci Lett 72:23–38

Foley SF (1988) The genesis of continental basic alkaline magmas – an interpretation in terms of redox melting. In: Oceanic and continental lithosphere: similarities and differences. Menzies MA, Cox KG (eds), J Petrol Spec Vol 1988, 139–161

Foley SF, Jenner GA, Jackson SE, Fryer BJ (1994) Trace element partition coefficients between phlogopite, clinopyroxene and matrix in an alkaline lamprophyre from Newfoundland, Canada. Mineral Mag 58A:280–281

Galer SJG, O'Nions RK (1986) Magmagenesis and the mapping of chemical and isotopic variations in the mantle. Chem Geol 56:45–61

Glahn A, Sachs PM, Achauer U (1992) A teleseismic and petrological study of the crust and upper mantle beneath the geothermal anomaly of Urach/SW Germany. Phys Earth Planet Inter 69:176–206

Griffiths RW, Campbell IH (1991) Interaction of mantle plume heads with the Earth's surface and onset of small-scale convection. J Geophys Res 96:18295–18310

Halliday AN, Dickin AP, Fallick AE, Fitton JB (1988) Mantle dynamics: Nd, Sr, Pb and O isotopic study of the Cameroon line Volcanic Chain. J Petrol 29:181–211

Halliday AN, Davidson JP, Holden P, De Wolf C, Lee DC, Fitton JG (1990) Trace-element fractionation in plumes and the origin of HIMU mantle beneath the Cameroon line. Nature 347:523–528

Hart SR (1984) A large-scale isotope anomaly in the Southern Hemisphere mantle. Nature 309:753–757

Hartmann G, Wedepohl KH (1990) Metasomatically altered peridotite xenoliths from the Hessian Depression (Northwest Germany). Geochim Cosmochim Acta 54:71–86

Hawkesworth CJ, Rogers NW, van Calsteren PWC, Menzies MA (1984) Mantle enrichment processes. Nature 311:331–335

Hawkesworth CJ, Kempton PD, Rogers NW, Ellam RM, Van Calsteren PW (1990) Continental mantle lithosphere and shallow level enrichment processes in the Earth's mantle. Earth Planet Sci Lett 96:256–268

Hegner E, Tatsumoto M (1989) Pb, Sr, and Nd isotopes in seamount basalts from the Juan de Fuca Ridge and Kodiak Bowie Seamount Chain, NE Pacific. J Geophys Res 94:17839–17846

Hegner E, Roddick JC, Fortier SM, Hulbert L (1995) Nd, Sr, Pb, Ar, and O isotopic systematics of Sturgeon Lake kimberlite, Saskatchewan, Canada: constraints on emplacement age, alteration, and source composition. Contrib Mineral Petrol (in press)

Hoernle K, Tilton G, Schmincke H-U (1991) Sr-Nd-Pb isotopic evolution of Gran Canaria: evidence for shallow enriched mantle beneath the Canary Islands. Earth Planet Sci Lett 106:44–63

Hofmann AW (1988) Chemical differentiation of the Earth: the relationship between mantle, continental crust and oceanic crust. Earth Planet Sci Lett 90:297–314

Hofmann AW, White WM (1982) Mantle plumes from ancient oceanic crust. Earth Planet Sci Lett 57:421–436

Hofmann AW, Jochum KPl, Seufert M, White WM (1986) Nb and Pb in oceanic basalts: new constraints on mantle evolution. Earth Planet Sci Lett 79:33–45

Irving AJ (1980) Petrology and geochemistry of composite ultramafic xenoliths in alkalic basalts and implications for magmatic processes in the mantle. Am J Sci 280A:389–426

Irving AJ, Frey FA (1984) Trace element abundances in megacrysts and their host basalts: constraints on partition coefficients and megacryst genesis. Geochim Cosmochim Acta 48:1201–1221

Jenner GA, Longerich HP, Jackson SE, Fryer BJ (1990) ICP-MS – a powerful tool for high precision trace-element analysis in Earth sciences: evidence from analysis of selected U.S.G.S. reference samples. Chem Geol 83:133–148

Jochum KP, Seufert HM, Spettel B, Palme H (1986) The solar system abundances of Nb, Ta, and Y and the relative abundances of refractory lithophile elements in differentiated planetary bodies. Geochim Cosmochim Acta 50:1173–1183

Jochum KP, McDonough WF, Palme H, Spettel B (1989) Compositional constraints on the continental lithospheric mantle from trace elements in spinel peridotite xenoliths. Nature 340:548–550

Jordan TH (1979) Mineralogies, densities, and seismic velocities of garnet lherzolites and their geophysical implications. In: Boyd FR, Meyer HOA (eds) The mantle sample: inclusions in kimberlites and other volcanics. American Geophys Union, Washington, DC, pp 1–14

Keller J, Brey G, Lorenz V, Sachs P (1990) Volcanism and petrology of the upper Rhinegraben (Urach-Hegau-Kaiserstuhl). Conference excursion volume 2 A, Int Volcanol Congr (IAVCEI), Mainz, Germany

Kempton PD, Harmon RS, Stosch HG, Hoefs J, Hawkesworth CJ (1988) Open system O-isotope behaviour and trace element enrichment in the sub-Eifel mantle. Earth Planet Sci Lett 89:273–287

Kober B, Lippolt HJ (1985) Pre-Hercynian mantle lead transfer to basement rocks as indicated by lead isotopes of the Schwarzwald crystalline, SW-Germany. I: The lead isotope distribution and its correlation. Contrib Mineral Petrol 90:12–171

Kramers JD, Betton PJ, Cliff RA, Seck HA, Sachtleben T (1981) Sr and Nd isotopic variations in volcanic rocks from the West Eifel and their significance (abs). Fortschr Mineral Beih 59:246–247

Kramm U, Wedepohl KH (1990) Tertiary basalts and peridotite xenoliths from the Hessian Depression (NW Germany), reflecting mantle compositions low in radiogenic Nd and Sr. Contrib Mineral Petrol 106:1–8

Liew TC, Hofmann AW (1988) Precambrian crustal components, plutonic associations, plate environment of the Hercynian foldbelt of central Europe: implications from a Nd and Sr isotopic study. Contrib Mineral Petrol 98:129–138

Lippolt HJ, Todt W, Baranyi I (1973) K-Ar ages of basaltic rocks from the Urach volcanic district, SW-Germany. Fortschr Mineral Beih 50:101–102

Lloyd FE, Bailey DK (1975) Light element metasomatism of the continental mantle: the evidence and consequences. Phys Chem Earth 9:389–416

McDonough WF, McCulloch MT, Sun SS (1985) Isotopic and geochemical systematics in Tertiary–Recent basalts from southeastern Australia and implications for the evolution of the subcontinental lithosphere. Geochim Cosmochim Acta 49: 2051–2067
McKenzie DP (1989) Some remarks on the movement of small melt fractions in the mantle. Earth Planet Sci Lett 95:53–72
McKenzie DP, O'Nions RK (1995) The source regions of ocean island basalts. J Petrol 36:133–160
Mengel K, Sachs PM, Stosch HG, Wörner G, Loock G (1991) Crustal xenoliths from Cenozoic volcanic fields of Western Germany: implications for structure and composition of the continental crust. Tectonophysics 195:271–289
Menzies M, Murthy VR (1980) Mantle metasomatism as a precursor to the genesis of alkaline magmas – isotopic evidence. Am J Sci 280 A:622–38
Menzies M, Rogers N, Tindle A, Hawkesworth CJ (1987) Metasomatic enrichment processes in lithospheric peridotites, an effect of asthenosphere-lithosphere interaction. In: Menzies M, Hawkesworth CJ (eds) Mantle metasomatism. Academic Press Geology Series, London, pp 313–361
Nelson DR, McCulloch MT, Sun SS (1986) The origins of ultrapotassic rocks as inferred from Sr, Nd and Pb isotopes. Geochim Cosmochim Acta 50:231–245
O'Reilly SY, Griffin WL, Ryan CG (1991) Residence of trace elements in metasomatized spinel lherzolite xenoliths: a proton-microprobe study. Contrib Mineral Petrol 109:98–113
Riley TR, Bailey DK, Lloyd FE, Fenwick CS, Palmer MR (1994) Carbonatite metasomatism in the Eifel (Germany) sub-continental lithosphere: geochemical and isotopic signature (abstract) . Mineral Mag 58A:776–777
Rogers NW, Hawkesworth CJ, Palacz ZA (1992) Phlogopite in the generation of olivine melilitites from Namaqualand, South Africa and implications for element fractionation processes in the upper mantle. Lithos 28:347–365
Rosenbaum JM (1993) Mantle phlogopite: a significant lead repository? Chem Geol 106:475–483
Sachs PM (1988) Untersuchungen zum Stoffbestand der tieferen Lithosphäre an Xenolithen südwestdeutscher Vulkane. Diss Inst Geophys Univ Stuttgart
Schilling J-G (1985). Upper mantle heterogeneities and dynamics. Nature 314:62–67
Schleicher H, Baumann A, Keller J (1991) Pb isotopic systematics of alkaline volcanic rocks and carbonatites from the Kaiserstuhl, Upper Rhine rift valley, F.R.G. Chem Geol 93:231–243.
Sleep NH (1984) Tapping of magmas from ubiquitous mantle heterogeneities: an alternative to mantle plumes? J Geophys Res 89:10029–10041
Stein M, Hofmann AW (1992) Fossil plume head beneath the Arabian lithosphere? Earth Planet Sci Lett 114:193–209
Stosch HG, Lugmair GW (1986) Trace element and Sr and Nd isotope geochemistry of peridotite xenoliths from the Eifel (West Germany) and their bearing on the evolution of the subcontinental lithosphere. Earth Planet Sci Lett 80:281–298
Stosch HG, Seck HA (1980) Geochemistry and mineralogy of two spinel peridotite suites from Dreiser Weiher, W. Germany. Geochim Cosmochim Acta 44:457–470
Sudo A, Tatsumi Y (1990) Phlogopite and K-amphibole in the upper mantle: implication for magma genesis in subduction zones. Geophys Res. Lett 17:29–32
Sun SS (1980) Lead isotopic study of young volcanic rocks from mid-ocean ridges, ocean islands and island arcs. Philos Trans R Soc London A 297:409–445
Sun SS (1989) Growth of lithospheric mantle. Nature 340:509–510
Sun SS, Hanson GN (1975) Origin of Ross Island basanitoids and limitations upon the heterogeneity of mantle sources for alkali basalts and nephelinites. Contrib Mineral Petrol 52:77–106
Sun SS, McDonough WF (1989) Chemical and isotopic systematics of oceanic basalts: implications for mantle composition and processes. In: Saunders AD, Norry M J (eds) Magmatism in the ocean, Geol Soc Spec Publ 42, pp 313–345
Vidal P, Postaire B (1985) Etude par la methode Pb-Pb de roches de haut grade metamorphique impliquees dans la chaine Hercynienne. Chem Geol 49:429–449
Vitrac AM, Albarede F, Allegre CJ (1981) Lead isotopic composition of Hercynian granitic K-feldspars constrains continental genesis. Nature 291:460–464
Von Engelhard W, Weiskirchner W (1963) Einführung zu den Exkursionen der Deutschen Mineralogischen Gesellschaft zu den Vulkanschloten der Schwäbischen Alb und dem Hegau. Fortschr Mineral 40:5–18
Walter HJ, Hegner E, Satir M (1994) Geochemistry of megacrysts and melilitites, Urach volcanic field, SW Germany: Tertiary Western European volcanic province. Int Volcanol Congr (IAVCEI), Ankara, Turkey
Weaver BL (1991a) Trace element evidence for the origin of ocean-island basalts. Geology 19:123–126
Weaver BL (1991b) The origin of ocean island basalt end-member compositions: trace element and isotopic constraints. Earth Planet Sci Lett 104:381–397
Wedepohl KH (1985) Origin of the Tertiary basaltic volcanism in the northern Hessian Depression. Contrib Mineral Petrol 89:122–143
Wedepohl KH, Gohn E, Hartmann G (1994) Cenozoic alkali basaltic magmas of western Germany and their products of differentiation. Contrib Mineral Petrol 115:252–278
White WM, Hofmann AW (1982) Sr and Nd isotope geochemistry of oceanic basalts and mantle evolution. Nature 296:821–825
White WM (1993) $^{238}U/^{204}Pb$ in MORB and open system evolution of the depleted mantle. Earth Planet Sci Lett 115:211–226
Wilson M, Downes H (1991) Tertiary-Quaternary extension related alkaline magmatism in Western and Central Europe. J Petrol 32:811–849
Wilson M, Rosenbaum JM, Dunworth EA (1995) Melilitites: partial melts of the thermal boundary layer? Contrib Mineral Petrol 119:181–196
Wimmenauer W (1974) The alkaline province of Central Europe and France. In: Sorensen H (ed): The alkaline rocks. John Wiley, London; pp 238–270
Witt G, Seck HA (1989) Origin of amphibole in recrystallized and porphyroclastic mantle xenoliths from the Rhenish Massif:implications for the nature of mantle metasomatism. Earth Planet Sci Lett 91:327–340
Wörner G, Zindler A, Staudigel H, Schmincke HU (1986) Sr, Nd and Pb isotope geochemistry of Tertiary and Quaternary alkaline volcanics from West Germany. Earth Planet Sci Lett 79:107–119
Ziegler PA (1992) European Cenozoic rift system. Tectonophysics 208:91–111
Zindler A, Hart SR (1986) Chemical geodynamics. Annu Rev Earth Planet Sci 14:493–571
Zindler A, Staudigel H, Batiza R (1984) Isotope and trace element geochemistry of young Pacific seamounts: implications for the scale of upper mantle heterogeneity. Earth Planet Sci Lett 70:175–195